



**HAL**  
open science

## Mother-plant-mediated pumping of zinc into the developing seed

Lene Irene Olsen, Thomas Hansen, Camille Larue, Jeppe Thulin Osterberg, Robert Hoffmann, Johannes Liesche, Ute Kramer, Suzy Surblé, Stéphanie Cadarsi, Vallerie Ann Samson, et al.

► **To cite this version:**

Lene Irene Olsen, Thomas Hansen, Camille Larue, Jeppe Thulin Osterberg, Robert Hoffmann, et al.. Mother-plant-mediated pumping of zinc into the developing seed. *Nature Plants*, 2016, 2 (5), 10.1038/nplants.2016.36 . hal-02325140

**HAL Id: hal-02325140**

**<https://hal.science/hal-02325140>**

Submitted on 10 Nov 2020

**HAL** is a multi-disciplinary open access archive for the deposit and dissemination of scientific research documents, whether they are published or not. The documents may come from teaching and research institutions in France or abroad, or from public or private research centers.

L'archive ouverte pluridisciplinaire **HAL**, est destinée au dépôt et à la diffusion de documents scientifiques de niveau recherche, publiés ou non, émanant des établissements d'enseignement et de recherche français ou étrangers, des laboratoires publics ou privés.

# Mother plant-mediated pumping of zinc into the developing seed

Lene Irene Olsen<sup>1,2</sup>, Thomas H. Hansen<sup>2</sup>, Camille Larue<sup>3,4</sup>, Jeppe Thulin Østerberg<sup>1,2</sup>, Robert D. Hoffmann<sup>1,2</sup>, Johannes Liesche<sup>2,5</sup>, Ute Krämer<sup>3</sup>, Suzy Surblé<sup>6</sup>, Stéphanie Cadarsi<sup>4</sup>, Vallerie Ann Samson<sup>7</sup>, Daniel Grolimund<sup>7</sup>, Søren Husted<sup>2</sup> and Michael Palmgren<sup>1,2,8\*</sup>

**1 Insufficient intake of zinc and iron from a cereal-based diet is one of the causes of “hidden hunger” (micronutrient deficiency), which affects some two billion people<sup>1,2</sup>. Identifying a limiting factor in the molecular mechanism of zinc loading into seeds is an important step towards determining the genetic basis for variation of grain micronutrient content and developing breeding strategies to improve this trait<sup>3</sup>. Nutrients are translocated to developing seeds at a rate that is regulated by transport processes in source leaves, in the phloem vascular pathway, and at seed sinks. Nutrients are released from a symplasmic maternal seed domain into the seed apoplast surrounding the endosperm and embryo by poorly understood membrane transport processes<sup>4–6</sup>. Plants are unique among eukaryotes in having specific P1B-ATPase pumps for the cellular export of zinc<sup>7</sup>. In *Arabidopsis*, we show that two zinc transporting P1B-ATPases actively export zinc from the mother plant to the filial tissues. Mutant plants that lack both zinc pumps accumulate zinc in the seed coat and consequently have vastly reduced amounts of zinc inside the seed. Blockage of zinc transport was observed both at high and low external zinc supplies. The phenotype was determined by the mother plant and is thus due to a lack of zinc pump activity in the seed coat and not in the filial tissues. The finding that P1B-ATPases are one of the limiting factors controlling the amount of zinc inside a seed is an important step towards combating nutritional zinc deficiency worldwide.**

In the quest to identify the membrane-bound transporters that deliver zinc into seeds, heavy metal-transporting P1B-ATPases, which belong to the family of P-type ATPases that actively transport ions and lipids across membranes, are promising candidates. In *Arabidopsis thaliana*, the P1B-ATPase subfamily consists of eight members, AtHMA1–8 (ref. 8). Whereas AtHMA2–4 transport divalent zinc and cadmium cations and AtHMA5–8 transport monovalent copper and silver cations, AtHMA1 has been implicated in the transport of a number of different cations including copper, silver, zinc and cadmium<sup>9,10</sup>. AtHMA3 is localized to the tonoplast and is involved in detoxification by sequestering excess amounts of zinc and cadmium into the vacuole<sup>11</sup>. AtHMA2 and AtHMA4 are structurally very similar to each other and have overlapping functions. Whereas the *hma2* and *hma4* single mutants have wild-type growth rates, the *hma2,hma4* double mutant shows a stunted growth phenotype that can only be rescued by zinc supplementation. Also, the *hma2,hma4* double mutant does

not set seed, a phenotype mainly ascribed to a defect in pollen development<sup>12</sup>. Both AtHMA2 and AtHMA4 have been localized to the plasma membrane and function as cellular zinc exporters<sup>12–14</sup>. Their involvement in xylem loading of zinc in roots is well known. They are both expressed in the root pericycle and xylem parenchyma cells and mutants lacking functional AtHMA2 and AtHMA4 accumulate zinc in the pericycle and endodermal cell layers, and exhibit reduced root-to-shoot translocation of zinc<sup>12,13</sup>. The finding that the zinc hyperaccumulator *Arabidopsis halleri* accumulates high levels of zinc in the shoot mainly because of the strongly enhanced expression of *AhHMA4*, caused by activating *cis*-regulatory mutations and gene copy number expansion<sup>15</sup>, emphasizes the role of HMA4 in the root-to-shoot translocation of zinc.

To test whether developing seeds depend on *AtHMA2* and *AtHMA4* for proper zinc unloading from the seed coat, we analysed the amount of zinc present in the maternal and filial parts of the seed, respectively, in wild-type and mutant seeds lacking functional *AtHMA2*, *AtHMA4*, or both. For this purpose, we developed an assay in which mature seeds are separated into seed coat (with the endosperm attached) and embryo fractions, and their respective metal contents are subsequently analysed by inductively coupled plasma mass spectrometry (ICPMS). All seeds used for this analysis were from plants grown side by side in soil watered with 3 mM ZnSO<sub>4</sub> twice a week, as these conditions were needed for the *hma2,hma4* double mutant to set seed. At this relatively high zinc supply, trafficking of zinc to the shoot did not differ between genotypes (Supplementary Fig. 1). We determined the total amounts of zinc, magnesium, phosphorus and manganese in batches of ten mature seeds, either intact or separated into seed coat and embryo fractions, using ICPMS. This revealed that the content of the different genotypes or between the content of intact seeds and the combined content of separated seeds for the tested elements showed little variation (Supplementary Fig. 2). As there was no difference between the weight of seeds of different genotypes and the combined weight of their separated parts (Supplementary Fig. 3a), loss of material during the separation procedure was negligible. However, the weight of any ten seeds was variable, which explains the variance seen for the total amounts of element. Instead of weighing samples before ICPMS, which could result in contamination, we used the ratio of seed coat weight to embryo weight as a reference point for normalizing data as it consistently was found to be very similar between and within genotypes (Supplementary Fig. 3b).

We found that in wild-type seeds most of the zinc was present in the embryo fraction (Fig. 1a). Conversely, in the *hma2,hma4* double

<sup>1</sup>Centre for Membrane Pumps in Cells and Disease-PUMPKIN, Danish National Research Foundation, Denmark. <sup>2</sup>Department of Plant and Environmental Sciences, University of Copenhagen, Thorvaldsensvej 40, DK-1871 Frederiksberg, Denmark. <sup>3</sup>Department of Plant Physiology, Ruhr University Bochum, Bochum, Germany. <sup>4</sup>ECOLAB, Université de Toulouse, CNRS, INPT, UPS, France. <sup>5</sup>College of Life Sciences, Northwest A&F University, Yangling, China. <sup>6</sup>LEEL, NIMBE-CEA-CNRS, Université Paris-Saclay, CEA Saclay, Gif-sur-Yvette Cedex, France. <sup>7</sup>MicroXAS beamline, Swiss Light Source, Villigen, Switzerland. <sup>8</sup>Institute of Environmental Medicine, Karolinska Institutet, SE-171 77 Stockholm, Sweden. \*e-mail: palmgren@plen.ku.dk

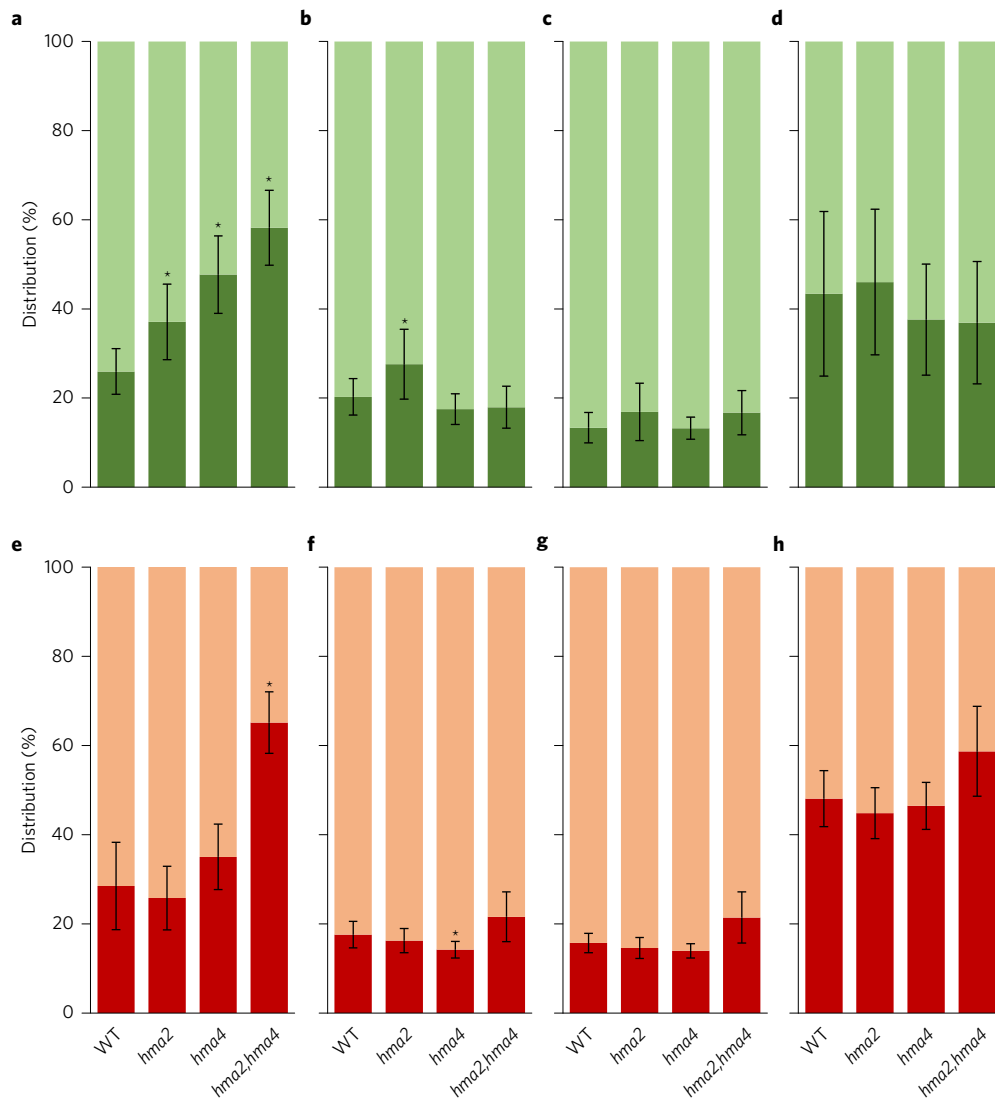


**Figure 1 | The distribution of zinc is shifted from the embryo to the seed coat of mature *hma2,hma4* seeds.** Microanalytical multi-elemental profiling of batches of ten seeds separated into seed coats and embryos. **a–d**, Distribution of elements in seeds from plants grown at high zinc supply (**a–d**) and plants grown at low zinc supply (**e–h**) (inflorescences of different genotypes had been grafted onto wild-type rootstocks). Bars represent the percentage of the total elemental content that is localized in the seed coat (dark green/red) and embryo (light green/red) fractions. **a,e**, Zinc; **b,f**, magnesium; **c,g**, phosphorus; and **d,h** manganese. Data are mean  $\pm$  s.d. of eight to ten replicates. Statistical analysis indicates significant difference from the wild type ( $^*p < 0.01$ ).

1 mutant, zinc accumulated in the seed coat fraction (Fig. 1a). In *hma2*  
 2 and *hma4* single mutants, only slightly more zinc accumulated in the  
 3 seed coat than the wild type, whereas the distribution of magnesium,  
 4 phosphorus and manganese did not show the same shift (Fig. 1a–d).  
 5 *hma2,hma4* double mutant plants did not develop seeds unless  
 6 supplemented with a high amount of zinc (3 mM ZnSO<sub>4</sub> twice a  
 7 week), but under these conditions overall zinc homeostasis of the  
 8 plant may be perturbed. To make the *hma2,hma4* double mutant  
 9 set seed under low zinc conditions, we grafted the mutant inflores-  
 10 cences onto wild-type rootstock. When the resulting plants were  
 11 grown under low external zinc conditions, *hma2,hma4* mutant  
 12 inflorescences produced seeds, and, compared with the seeds of  
 13 plants grown under high zinc conditions, contained a much lower  
 14 zinc content (reduced from around 50–10 ng for 10 seeds,  
 15 Supplementary Fig. 4). Under these conditions, seeds of *hma2*,  
 16 *hma4* double mutant inflorescences accumulated zinc in the seed  
 17 coat (Fig. 1e). This demonstrates that the *hma2,hma4* double  
 18 mutant fails to direct zinc towards the embryo both under high  
 19 and low external zinc supplies. By contrast, no shift in zinc

distribution was seen for the *hma2* and *hma4* single mutants at a  
 20 low zinc supply (Fig. 1e). 21

To confirm that HMAs are required for export of zinc from  
 22 the maternal to the filial parts of seeds, we employed micro-X-ray  
 23 fluorescence ( $\mu$ XRF) and micro-particle-induced X-ray emission  
 24 ( $\mu$ PIXE) coupled to micro-Rutherford backscattering spectroscopy  
 25 ( $\mu$ RBS) to obtain spatially resolved images of the distribution of  
 26 zinc in wild-type and mutant seeds.  $\mu$ PIXE/RBS also allows for  
 27 quantification of elemental concentrations in the seed sections. 28  
 For these experiments we obtained seeds from intact plants grown  
 29 with zinc supplementation. Our analysis of  $\mu$ XRF and  $\mu$ PIXE/RBS  
 30 maps of all together seven replicate sections imaged per genotype  
 31 indicated that the spatial distribution of zinc was consistently  
 32 altered in the *hma4* and *hma2,hma4* mutants compared with the  
 33 wild type (Fig. 2, Supplementary Fig. 5 and Supplementary  
 34 Table 1). In wild-type seeds, the distribution of elements was essen-  
 35 tially as reported earlier<sup>16,17</sup>. Iron was found to accumulate in the  
 36 provascular strands, manganese surrounded these strands on the  
 37 lower side of the cotyledons and calcium was enriched in the seed  
 38 39

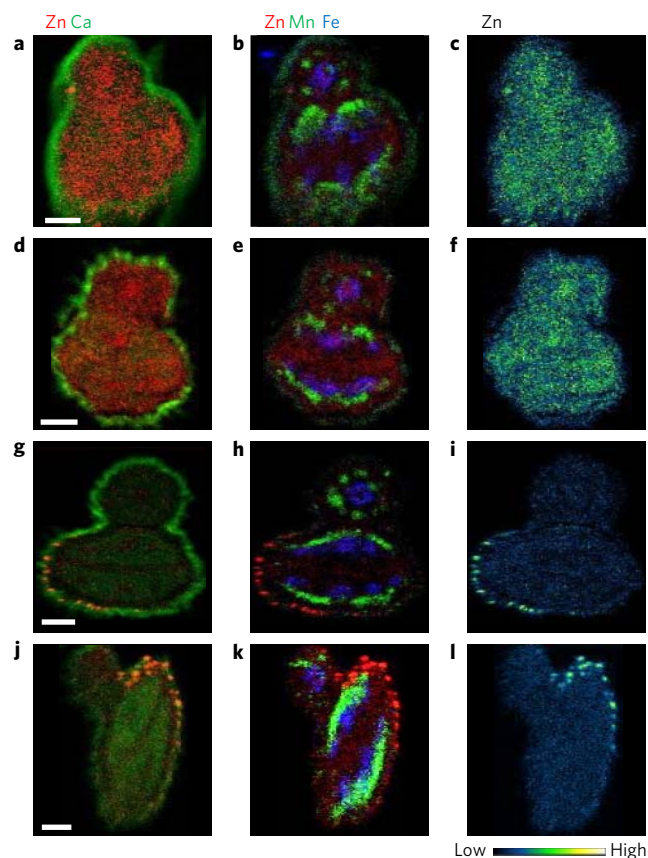


**Figure 2 | Zinc accumulates in the seed coat of mature *hma4* and *hma2, hma4* mutant seeds. a–l,  $\mu$ PIXE/RBS elemental profiles of transverse sections of seeds from wild-type (a–c), *hma2* mutant (d–f), *hma4* mutant (g–i) and *hma2,hma4* (j–l) double mutant plants grown at high zinc supply. a,d,g,j, Two-colour maps showing zinc (Zn) distribution in red and calcium (Ca) distribution in green. b,e,h,k, Three-colour maps showing zinc (Zn) distribution in red, manganese (Mn) distribution in green and iron (Fe) distribution in blue. c,f,i,l, Temperature colour maps displaying zinc distribution. Scale bars, 50  $\mu$ m.**

1 coat and showed an even distribution in the embryo, as did zinc  
2 (Fig. 2a–c). The pattern of zinc distribution in seeds of the *hma2*  
3 single mutant was similar to that of the wild-type (Fig. 2d–f). By  
4 contrast, zinc distribution was far more uneven across sections of  
5 seeds from both the *hma4* single mutant (Fig. 2g–i) and the  
6 *hma2,hma4* double mutant (Fig. 2j–l). In these mutants, the zinc  
7 signal was reduced in the embryo. By contrast, very high levels of  
8 zinc accumulated in the seed coat, with the frequency of high-  
9 intensity zinc hot spots gradually declining with increasing distance  
10 from the hilum inside the seed coat. There were no consistent  
11 changes in the distribution of other elements, such as calcium,  
12 iron and manganese, among the replicate sections analysed (Fig. 2  
13 and Supplementary Fig. 5).

14 To determine whether the ability to provide the embryo with zinc  
15 was a maternal property, we performed crosses between wild-type or  
16 *hma2,hma4* mother plants and wild-type or *hma2,hma4* pollen.  
17 Wild-type plants always produced seeds with an even distribution  
18 of zinc in the embryo, regardless of whether they had been fertilized  
19 with *hma2,hma4* or wild-type pollen. By contrast, mother plants  
20 with a *hma2,hma4* genotype always produced seeds that accumu-  
21 lated zinc in the seed coat, regardless of the genotype of the  
22 pollen (Figs. 3, 4 and Supplementary Table 2). This demonstrates  
23 that the observed accumulation of zinc in the seed coat is due to the  
24 lack of AtHMA2 and AtHMA4 in the seed coat itself. Taken together,

our ICPMS data in combination with  $\mu$ XRF and  $\mu$ PIXE/RBS  
mapping of elemental distribution suggest that cellular export of  
zinc towards the endosperm and embryo is blocked without the  
combined function of AtHMA2 and AtHMA4 in the seed coat.

Genome-wide gene activity profiling suggests that AtHMA2 and  
AtHMA4 are both expressed in developing seeds<sup>18</sup>, (Supplementary  
Fig. 6). To confirm the expression of AtHMA2 and AtHMA4 at this  
location, we generated transgenic plants expressing  $\beta$ -glucuronidase  
(GUS) and investigated the cell-specific expression of the GUS  
reporter using whole-mount confocal imaging. The AtHMA2 pro-  
moter was active throughout the seed, including both the seed  
coat and embryo, whereas AtHMA4 was expressed in the innermost  
cell layer of the seed coat surrounding the endosperm (the endo-  
thelium), in the chalazal region, and also in the embryo (Fig. 5d,e).  
This expression pattern was detected at all developmental stages  
(data not shown). When green fluorescent protein (GFP) was  
fused to the first half of AtHMA4 (HMA4-4TM-GFP) and the  
resulting construct was expressed under the control of the HMA4  
promoter in transgenic plants, we found GFP expression to be  
strong in the endothelium (Fig. 5f,g). This is consistent with the  
finding that, in the maternal tissues of developing seeds, AtHMA4  
is specifically expressed in the seed coat endothelium.

On the basis of our results, we suggest a model in which  
AtHMA2 and AtHMA4 are involved in the export of zinc from  
the mother plant seed coat to the filial tissues. The phloem is a  
long-distance vascular transport system in plants that transports  
nutrients to reproductive tissues. In *Arabidopsis* seeds, the phloem  
is symplastically connected to the seed coat. However, for nutrients  
to proceed further into filial tissues, apoplastic barriers have to be  
crossed, which requires transport across biological membranes<sup>4</sup>,  
and for zinc export against the inside-negative membrane potential.  
In the seed coat of the developing seed, an apoplastic barrier is  
present between the outer and inner integument, as well as  
between the inner integument and the endosperm, and between  
the endosperm and the embryo<sup>4</sup>. Whereas AtHMA2 was expressed  
in all integuments, AtHMA4 was mainly expressed in the innermost  
layer of the seed coat, the endothelium. Thus, AtHMA4 is a prime  
candidate for mediating the post-phloem translocation of zinc from  
the seed coat and into the endosperm cavity. The importance of  
AtHMA4 in this process is evident at a high zinc supply as, in the  
*hma4* mutant background, zinc accumulates in the seed coat, as  
shown by both ICPMS and  $\mu$ XRF/ $\mu$ PIXE. This phenotype is even  
stronger in the *hma2,hma4* double mutant at both a high and low  
zinc supply, which suggests that AtHMA2 also contributes to this  
process. The fact that zinc is present in the embryo even in the  
*hma2,hma4* double mutant indicates that other transporters exist  
in the seed coat that are able to export zinc into the endosperm  
cavity. A similar phenomenon is seen in the root, where zinc is  
loaded into the xylem even in the *hma2,hma4* double mutant<sup>12,13</sup>,  
a transport that at least partially seems to be mediated by the  
putative transporter AtPCR2 (ref. 19). However, this transport is  
only efficient at high zinc concentrations, which suggests that  
these secondary active transporters have a lower zinc affinity than  
do AtHMA2/4.

AtHMA2 and AtHMA4 belong to the P1B-2 subgroup of heavy  
metal ATPases, which are common in prokaryotes and plants but  
absent in animals<sup>7</sup>. Plant cells have substantially higher inside-  
negative membrane potentials than do animal cells<sup>20</sup>, which may  
be a reason why export of this micronutrient from plant cells  
cannot be sustained by proton antiporters alone when zinc is limit-  
ing, but requires the contribution of primary active transporters.  
The AtHMA2/4 homologue in *Hordeum vulgare* (barley) is  
HvHMA2, which functions as a plasma membrane-localized zinc  
exporter<sup>21</sup>. Expression analysis of laser capture microdissected  
developing barley grain showed that HvHMA2 is predominantly  
expressed in the nucellar projection transfer cells<sup>22</sup>, which



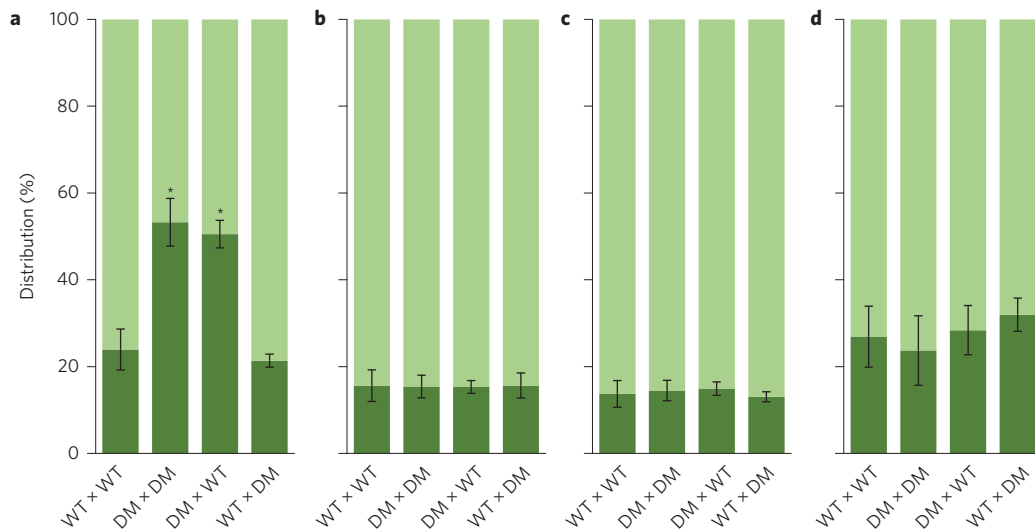


**Figure 3 | Lack of zinc pumps in the seed coat but not in filial tissues blocks zinc loading into seeds.** Microanalytical multi-elemental profiling of batches of ten seeds separated into seed coats and embryos. Bars represent the percentage of the total elemental content that is localized in the seed coat (dark green) and embryo (light green) fractions of seeds from crosses of plants grown at high zinc supply. Notations represent mother plant  $\times$  pollen donor. WT, wild type; DM, *hma2,hma4* double mutant. **a**, Zinc; **b**, magnesium; **c**, phosphorus; and **d**, manganese. Data are means  $\pm$  s.d. of eight to ten replicates, WT  $\times$  DM of three replicates. Statistical analysis indicates significant difference from the wild type ( $*p < 0.01$ ).

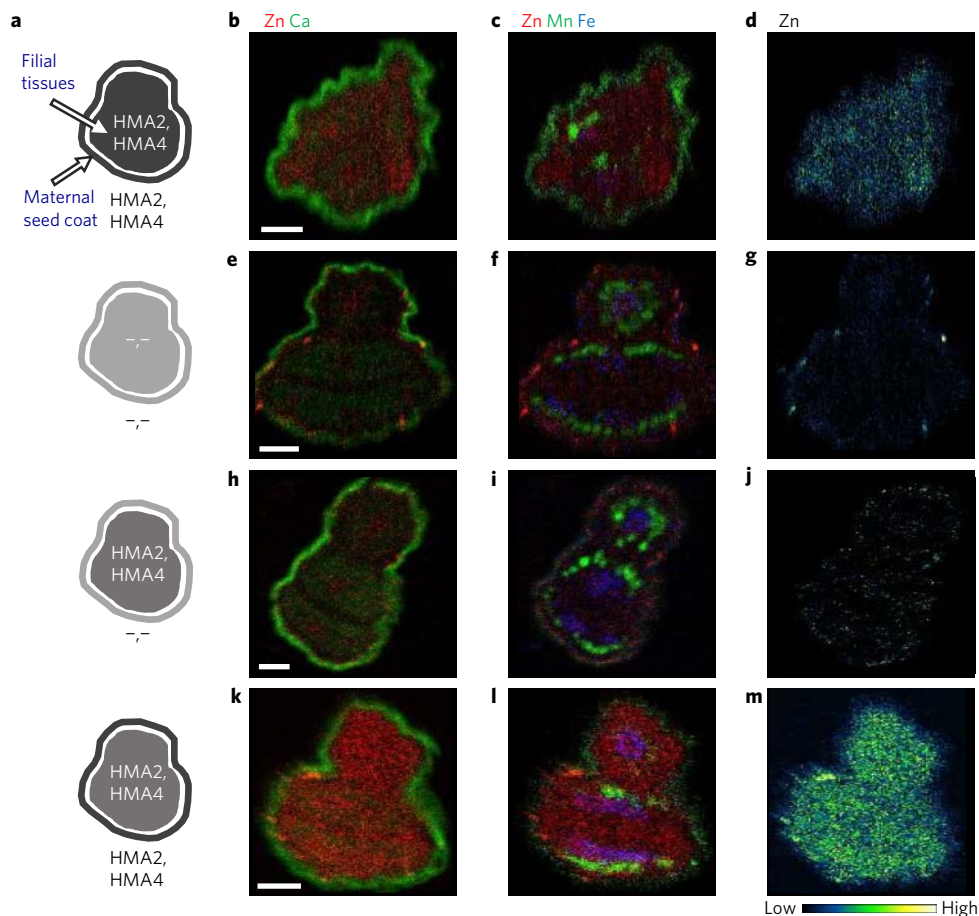


**Figure 4 | Zinc export from the seed coat to filial tissues depends on zinc pumps in maternal tissues.**  $\mu$ PIXE/RBS elemental profiles of transverse sections of seeds from crosses of plants grown at high zinc supply. **a**, Pictograms indicate presence of AtHMA2 and AtHMA4. Dark grey, AtHMA2 and AtHMA4 present (homozygous WT); intermediate grey, AtHMA2 and AtHMA4 present (hemizygous); light grey, AtHMA2 and AtHMA4 absent (homozygous *hma2,hma4*). **b-m**, Colour maps showing distribution of elements. Two-colour maps showing zinc (Zn) distribution in red and calcium (Ca) distribution in green (**b,e,h,k**). Three-colour maps showing zinc (Zn) distribution in red, manganese (Mn) distribution in green and iron (Fe) distribution in blue (**c,f,i,l**). Temperature colour maps displaying zinc distribution (**d,g,j,m**). Scale bars, 50  $\mu$ m.

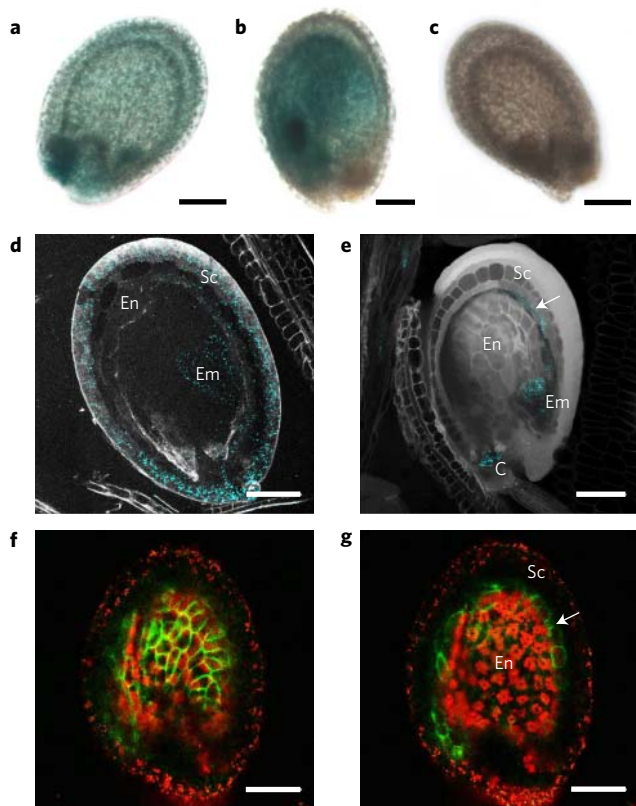


**Figure 5 | *AtHMA2* and *AtHMA4* are expressed in developing seeds.** **a–e**, Histochemical staining for GUS activity in developing seeds harbouring reporter gene fusions of the *AtHMA2* promoter (**a,d**) and *AtHMA4* promoter (**b,e**). (**c**) Wild-type seed. The images show whole seeds (**a–c**) and confocal laser scanning optical sections of modified pseudo-Schiff propidium iodide (mPS-PI)-stained seeds (**d,e**). **f–g**, Two different confocal laser scanning optical sections of the same developing seed expressing a fusion between a part of *AtHMA4* and GFP under the control of the *AtHMA4* promoter. Green, GFP fluorescence; red, autofluorescence; C, chalazal region; En, endosperm; Em, embryo; Sc, seed coat. The arrow indicates the endothelium. Scale bars, 100  $\mu\text{m}$ .

1 correspond to the endothelium of the seed coat in *Arabidopsis*. The  
 2 homologue in rice is OsHMA2, which functions as a zinc transporter  
 3 involved in the root-to-shoot translocation of zinc<sup>23–25</sup>. Whether  
 4 HvHMA2 and OsHMA2 also play crucial roles in the developing  
 5 grain remains to be investigated; however, it is conceivable that  
 6 they would have similar functions as *AtHMA2–4*. In efforts to  
 7 increase the zinc translocation capacity of plants, *HMA4* from  
 8 either *A. thaliana* or *A. halleri* has been transgenically expressed  
 9 in *Arabidopsis*, *Nicotiana tabacum* (tobacco) and *Solanum lycopersicum*  
 10 (tomato), but with inconsistent results<sup>14,15,26–29</sup>. Notably, none  
 11 of these studies made use of endogenous *HMA* promoters. Cellular  
 12 mislocalization of *HMA4* is likely to cause undesired export of zinc  
 13 and interrupt the natural flow of zinc within the plant body. To  
 14 attain this goal, the natural expression patterns of *HMA2* or  
 15 *HMA4* should be retained. The finding that localization of  
 16 *AtHMA4* to the seed coat endothelium is crucial for export of  
 17 zinc into the seed provides us with an essential handle in breeding  
 18 efforts aimed at fighting hidden hunger.

## 19 Methods

20 **Plant material.** *A. thaliana* Columbia-0 was used as the wild type. The single  
 21 mutants *hma2-4* and *hma4-2* and the double mutant *hma2-4,hma4-2* were as  
 22 described<sup>15</sup>. Plant growth, cloning and plant transformation procedures for creating  
 23 transgenic GUS and GFP plants are described in the Supplementary Methods.

**Multi-elemental analysis.** Samples were prepared for multi-elemental analysis as  
 24 described in the Supplementary Materials and Methods. Multi-elemental analysis of  
 25 seeds was performed using flow injection analysis (FIA) with the following  
 26 parameters: ICPMS was set up with an injection volume of 50  $\mu\text{l}$ , a flow of  
 27 0.2 ml  $\text{min}^{-1}$  and a mobile phase of 3.5%  $\text{HNO}_3$ . For the FIA, a Thermo ICS  
 28 5,000 DP pump and an Ultimate 3,000 UHPLC auto-sampler (Thermo Scientific)  
 29 were used. A triple quad ICPMS (Model 8,800, Agilent Technologies) equipped with  
 30 an Ari Mist HP nebulizer (Burgener Research International) was used. The ICPMS  
 31 instrument was run in collision mode using helium as the collision gas; zinc,  
 32 manganese, magnesium and phosphorus were analysed at  $m/z$  ratios of 66, 55, 24  
 33 and 31, respectively. Data were acquired and processed using the MassHunter 4.1  
 34 Chromatographic software package. For external calibration, a custom-made  
 35 multi-element standard was used (P/N 4400-ICP-MSCS, CPI International). The  
 36 standard is non-equimolar and corresponds to the ratio between elements typically  
 37 found in plants. The digestion procedure and elemental analysis were validated using  
 38 the certified reference material (CRM) NIST 1,515 Apple Leaf (National Institute  
 39 of Standard and Technology). For magnesium, phosphorus, manganese and zinc,  
 40 an accuracy of within  $\pm 10\%$  was obtained for samples ranging in size from 200 to  
 41 2,000  $\mu\text{g}$  ( $n = 8$ ). *Arabidopsis* seeds were analysed in sample batches of ten intact  
 42 seeds or ten fractionated seeds divided into seed coats and embryos, typically  
 43 weighing from 50 to 200  $\mu\text{g}$ . The elemental concentrations in these small sample  
 44 batches were reported as nanograms of element per ten seeds. The combined masses  
 45 of the elements measured in the seed coat plus embryo were within  $\pm 10\%$  of the  
 46 masses determined in the whole seed, indicating a negligible level of sample loss or  
 47 contamination during the analytical procedure.  
 48

**$\mu\text{PIXE/RBS}$ .** Seeds were immersed in a droplet of resin (OCT, Tissue Teck Sakura)  
 49 and immediately cryo-fixed by plunging into isopentane cooled with liquid nitrogen.  
 50 Seed cross-sections (30  $\mu\text{m}$ ) were done using a cryo-microtome (Leica) and freeze-  
 51 dried (48 h,  $-52^\circ\text{C}$ , 0.01 mbar). Samples were analysed under vacuum at the Atomic  
 52 Energy Commission nuclear microprobe (Saclay, France). The beamline was  
 53 operated with a proton source at 3.03 MeV, with a beam focused to  $3 \times 3 \mu\text{m}^2$  and a  
 54 current intensity of 500 pA.  
 55

**GUS analysis.** Developing siliques were slit open longitudinally and stained for 3 h  
 56 at  $37^\circ\text{C}$  in GUS staining solution following 5 min of vacuum treatment. The GUS  
 57 staining solution contained 50 mM  $\text{NaPO}_4$  at pH 7.2, 3 mM ferricyanide, 3 mM  
 58 ferrocyanide, 0.4% Tween20 and 2 mM X-GlcA. The samples were then cleared in  
 59 98% ethanol or fixed in fixing solution (50% methanol and 10% acetic acid) for  
 60 modified pseudo-Schiff propidium iodide (mPS-PI) staining. The mPS-PI staining  
 61 was as described<sup>30</sup>. Samples were examined using a Leica TCS SP5X confocal  
 62 microscope with a  $20\times$  water immersion objective in sequential mode and were  
 63 excited with a 488 nm argon laser. The propidium iodide emission signal was  
 64 collected at 520–720 nm and the GUS reflection signal was collected at 485–491 nm  
 65 (using the AOBs reflection mode). Cleared developing seeds were imaged by  
 66 brightfield microscopy (Leica DM 5000B).  
 67

**GFP analysis.** To image developing seeds, siliques were slit open longitudinally and  
 68 seeds were gently removed using a scalpel, mounted on a microscope slide and  
 69 imaged immediately. Fluorescence microscopy was performed using an inverted  
 70 point-scanning confocal microscope (Leica TCS SP5 II) with a  $20\times$  water immersion  
 71 objective. Samples were excited with a 488 nm argon laser; emission was collected at  
 72 500–530 nm for GFP and at 660–700 nm for chlorophyll autofluorescence.  
 73

Received 17 February 2015; accepted 29 February 2016;

published xx xx 2016

## References

1. Wessells, K. R. & Brown, K. H. Estimating the global prevalence of zinc  
 77 deficiency: results based on zinc availability in national food supplies and the  
 78 prevalence of stunting. *PLoS One* **7**, e50568 (2012).  
 79
2. von Grebmer, K. *et al.* *Global hunger index: the challenge of hidden hunger*  
 80 (International Food Policy Research Institute, 2014).  
 81
3. Palmgren, M. G. *et al.* Zinc biofortification of cereals: problems and solutions.  
 82 *Trends Plant Sci.* **13**, 464–473 (2008).  
 83
4. Stadler, R., Lauterbach, C. & Sauer, N. Cell-to-cell movement of green  
 84 fluorescent protein reveals post-phloem transport in the outer integument and  
 85 identifies symplastic domains in *Arabidopsis* seeds and embryos. *Plant Physiol.*  
 86 **139**, 701–712 (2005).  
 87
5. Zhang, W. *et al.* Nutrient loading of developing seeds. *Funct. Plant Biol.* **34**,  
 88 314–331 (2007).  
 89
6. Radchuk, V. & Borisjuk, L. Physical, metabolic and developmental functions of  
 90 the seed coat. *Front. Plant Sci.* **5**, 510 (2014).  
 91
7. Williams, L. E. & Mills, R. F. P1B-ATPases – an ancient family of transition  
 92 metal pumps with diverse functions in plants. *Trends Plant Sci.* **10**,  
 93 491–502 (2005).  
 94
8. Baxter, I. *et al.* Genomic comparison of P-type ATPase ion pumps in  
 95 *Arabidopsis* and rice. *Plant Physiol.* **132**, 618–628 (2003).  
 96

- 1 9. Kim, Y.-Y. *et al.* AtHMA1 contributes to the detoxification of excess Zn(II) in  
2 *Arabidopsis*. *Plant J.* **58**, 737–753 (2009).
- 3 10. Seigneurin-Berny, D. *et al.* HMA1, a new Cu-ATPase of the chloroplast  
4 envelope, is essential for growth under adverse light conditions. *J. Biol. Chem.*  
5 **281**, 2882–2892 (2006).
- 6 11. Morel, M. *et al.* AtHMA3, a P(1B)-ATPase allowing Cd/Zn/Co/Pb vacuolar  
7 storage in *Arabidopsis*. *Plant Physiol.* **149**, 894–904 (2009).
- 8 12. Hussain, D. *et al.* P-type ATPase heavy metal transporters with roles in essential  
9 zinc homeostasis in *Arabidopsis*. *Plant Cell* **16**, 1327–1339 (2004).
- 10 13. Sinclair, S. A. *et al.* The use of the zinc-fluorophore, Zinpyr-1, in the study of  
11 zinc homeostasis in *Arabidopsis* roots. *New Phytol.* **174**, 39–45 (2007).
- 12 14. Vernet, F. *et al.* Overexpression of AtHMA4 enhances root-to-shoot  
13 translocation of zinc and cadmium and plant metal tolerance. *FEBS Lett.* **576**,  
14 306–312 (2004).
- 15 15. Hanikenne, M. *et al.* Evolution of metal hyperaccumulation required *cis*-  
16 regulatory changes and triplication of HMA4. *Nature* **453**, 391–396 (2008).
- 17 16. Kim, S. A. *et al.* Localization of iron in *Arabidopsis* seed requires the vacuolar  
18 membrane transporter VIT1. *Science* **314**, 1295–1298 (2006).
- 19 17. Schnell Ramos, M. *et al.* Using  $\mu$ PIXE for quantitative mapping of metal  
20 concentration in *Arabidopsis thaliana* seeds. *Front Plant Sci.* **4**, 168 (2013).
- 21 18. Le, B. H. *et al.* Global analysis of gene activity during *Arabidopsis* seed  
22 development and identification of seed-specific transcription factors. *Proc. Natl*  
23 *Acad. Sci. USA* **107**, 8063–8070 (2010).
- 24 19. Song, W.-Y. *et al.* *Arabidopsis* PCR2 is a zinc exporter involved in both zinc  
25 extrusion and long-distance zinc transport. *Plant Cell* **22**, 2237–2252 (2010).
- 26 20. Morth, J. P. *et al.* A structural overview of the plasma membrane Na<sup>+</sup>,K<sup>+</sup>-ATPase  
27 and H<sup>+</sup>-ATPase ion pumps. *Nature Rev. Mol. Cell Biol.* **12**, 60–70 (2011).
- 28 21. Mills, R. F. *et al.* HvHMA2, a P1B-ATPase from barley, is highly  
29 conserved among cereals and functions in Zn and Cd transport. *PLoS One* **7**,  
30 e42640 (2012).
- 31 22. Tauris, B. *et al.* A roadmap for zinc trafficking in the developing barley grain  
32 based on laser capture microdissection and gene expression profiling. *J. Exp. Bot.*  
33 **60**, 1333–1347 (2009).
- 34 23. Satoh-Nagasawa, N. *et al.* Mutations in rice (*Oryza sativa*) Heavy Metal ATPase  
35 2 (OsHMA2) restrict the translocation of zinc and cadmium. *Plant Cell Physiol.*  
36 **53**, 213–224 (2012).
- 37 24. Takahashi, R. *et al.* The OsHMA2 transporter is involved in root-to-shoot  
38 translocation of Zn and Cd in rice. *Plant Cell Environ.* **35**, 1948–1957 (2012).
- 39 25. Yamaji, N. *et al.* Preferential delivery of zinc to developing tissues in rice is  
40 mediated by P-type heavy metal ATPase OsHMA2. *Plant Physiol.*  
41 **162**, 927–939 (2013).
26. Barabasz, A. *et al.* Metal accumulation in tobacco expressing *Arabidopsis halleri*  
42 metal hyperaccumulation gene depends on external supply. *J. Exp. Bot.* **61**,  
43 3057–3067 (2010).
- 44 27. Siemianowski, O. *et al.* Expression of the P1B-type ATPase AtHMA4 in tobacco  
45 modifies Zn and Cd root to shoot partitioning and metal tolerance. *Plant*  
46 *Biotechnol. J.* **9**, 64–74 (2011).
- 47 28. Cun, P. *et al.* Modulation of Zn/Cd P1B2-ATPase activities in *Arabidopsis*  
48 impacts differently on Zn and Cd contents in shoots and seeds. *Metallomics* **6**,  
49 2109–2916 (2014).
- 50 29. Kendziorek, M. *et al.* Approach to engineer tomato by expression of AtHMA4 to  
51 enhance Zn in the aerial parts. *J. Plant Physiol.* **171**, 1413–1422 (2014).
- 52 30. Truernit, E. *et al.* High-resolution whole-mount imaging of three-dimensional  
53 tissue organization and gene expression enables the study of phloem  
54 development and structure in *Arabidopsis*. *Plant Cell* **20**, 1494–1503 (2008).
- 55

### Acknowledgements

The authors thank C.S. Cobbett (University of Melbourne) for providing *hma2-4*, *hma4-2*, and *hma2-4*, *hma4-2* mutant seeds and the Centre for Advanced Bioimaging (University of Copenhagen) for support and use of microscopes. We acknowledge the Paul Scherrer Institut, Villigen, Switzerland, for providing the synchrotron radiation beamtime at beamline MicroXAS of the SLS. The research leading to these results was funded by the University of Copenhagen's Excellency Programme KU2016, the People Programme (Marie Curie Actions) of the European Union's Seventh Framework Programme (FP7/2007-2013) under REA grant agreement no. PIEF-GA-2012-331680, and the European programme CALIPSO (no. 312284).

### Author contributions

L.I.O., T.H.H., C.L., J.T.H., J.L., S.S., S.C. and V.S. performed the experimental work. L.I.O., T.H.H., C.L., R.D.H., J.L., S.S., U.K., S.H. and M.P. performed data analysis. D.G., U.K., S.H. and M.P. oversaw project planning. L.I.O. and M.P. wrote the manuscript. All authors discussed the results and commented on the manuscript.

### Additional information

Supplementary information is available online. Reprints and permissions information is available online at [www.nature.com/reprints](http://www.nature.com/reprints). Correspondence and requests for materials should be addressed to M.P.

### Competing interests

The authors declare no competing financial interests.

Journal: NPLANTS

Article ID: nplants-2016-36

Article Title: Mother plant-mediated pumping of zinc into the developing seed

Author(s): Lene Irene Olsen *et al.*

Query Nos.	Queries	Response
1	For all author addresses, please provide post/zip code	
2	What does HMA stand for?	
3	Ref 17: Please provide final page number if article is greater than one page.	
4	Figure 4: please check edits to the caption	